

Stability of the ω structure of transition elements

Yuji Ikeda^{1,*} and Isao Tanaka^{1,2,3,4,†}

¹*Center for Elements Strategy Initiative for Structure Materials (ESISM), Kyoto University, Kyoto 606-8501, Japan*

²*Department of Materials Science and Engineering, Kyoto University, Kyoto 606-8501, Japan*

³*Center for Materials Research by Information Integration,*

National Institute for Materials Science (NIMS), Tsukuba 305-0047, Japan

⁴*Nanostructures Research Laboratory, Japan Fine Ceramics Center, Nagoya 456-8587, Japan*

(Dated: July 12, 2021)

Properties of the ω structure are investigated for 27 transition elements from the viewpoints of thermodynamical and mechanical stability based on first-principles calculations. The thermodynamical stability of the ω structure is compared with those for the body-centered cubic (BCC), face-centered cubic (FCC), and hexagonal close-packed (HCP) structures. Similarly to the case of those popular crystal structures, the occupation number for d orbitals is found to roughly determine relative energy and volume of the nonmagnetic (NM) ω structure. For the group 4 elements (Ti, Zr, and Hf), the ω structure is almost the lowest in energy among the investigated crystal structures and is also mechanically stable. The ω structure of the group 7 elements (Mn, Tc, and Re) is also mechanically stable. The ω Fe is found to exhibit a complicated magnetic state that is different from the ferromagnetic (FM) and NM ones. This magnetic state is the most favorable among the investigated magnetic states. The ω Fe in this magnetic state is also mechanically stable. Energies of binary alloys composed of the elements in the group 4 and those in the groups 5 and 6 are estimated by linear interpolation, and most of the alloys show concentration ranges where the ω structure is the lowest in energy among the investigated crystal structures.

PACS numbers: 71.20.Be, 61.50.-f, 71.15.Mb, 63.20.-e, 63.20.dk

I. INTRODUCTION

The ω structure is included in the hexagonal crystal system with the space group of $P6/mmm$ (No. 191). It was first reported for Ti-Cr alloys, and its relation to the brittleness of the alloys was discussed [1]. The ω structure is observed for elemental Ti [2], Zr [2], and Hf [3, 4] under high pressure. Ti and Zr can hold the ω structure also after removing the pressure [2]. As well as the pure elements, the ω structure is observed for alloys based on the group 4 elements, namely Ti-[1, 5–10], Zr-[6, 11, 12], and Hf-[13] based alloys. In addition, it has been reported that the ω structure is formed in elemental Ta and Ta-W alloys by applying shock pressure [14] and in elemental Mo after high-pressure torsion [15]. Several experimental reports have recently claimed that the ω structure can be found also in steels, i.e., Fe-C-based alloys [16, 17]. Structures based on the ω lattice, where constituent elements occupy the same atomic sites as the ω structure with atomic orderings, have also been observed in experiments for alloys such as Cu-Zn [18], Cu-Mn-Al [19], Ni-Al [20], Fe-Ni-Co-Mo [21], Fe-Mn-Co-Mo [22], and Fe-Ni-Mo [23] alloys.

The ω structure can be obtained via collective motion of atoms from the body-centered cubic (BCC) [24], hexagonal-close packed (HCP) [5, 25, 26], and face-centered cubic (FCC) [27] structures. It is, therefore, suggested that the ω structure can be the transition state

of a transformation pathway between these popular crystal structures. Togo and Tanaka have actually revealed that the ω structure for Cu can be the transition state of a BCC-FCC transformation pathway based on a systematic search algorithm for transformation pathways [27]. Ikeda *et al.* have also pointed out that the ω structure for Fe acts as the transition state of the pressure-induced phase transition between the high-temperature paramagnetic (PM) BCC and PM FCC structures [28]. These results imply that the ω structure is important not only for the metals and the alloys that form the ω structure but also for general metallic systems to understand mechanisms of phase transitions. However, systematic knowledge of the ω structure for metallic systems is still missing.

It is interesting that the elements in the groups 5 and 6 such as V, Cr, Nb, and Mo are included in most of the alloys based on the group 4 elements that form the ω structure. For these alloys, the ω structure is observed in a concentration range where the group 4 elements are rich. These experimental facts imply that interactions between the group 4 elements and those in the groups 5 and 6 have essential roles to form the ω structure. To our best knowledge, however, no detailed and systematic investigations have been accomplished into this issue.

In this study, properties of the ω structure are systematically investigated for 27 transition elements from the viewpoints of thermodynamical and mechanical stability based on first-principles calculations. The thermodynamical stability of the ω structure is compared with those of the BCC, FCC, and HCP structures. The mechanical stability of the ω structure is investigated in terms of phonon frequencies. We also investigate thermo-

* ikeda.yuji.6m@kyoto-u.ac.jp

† tanaka@cms.mtl.kyoto-u.ac.jp

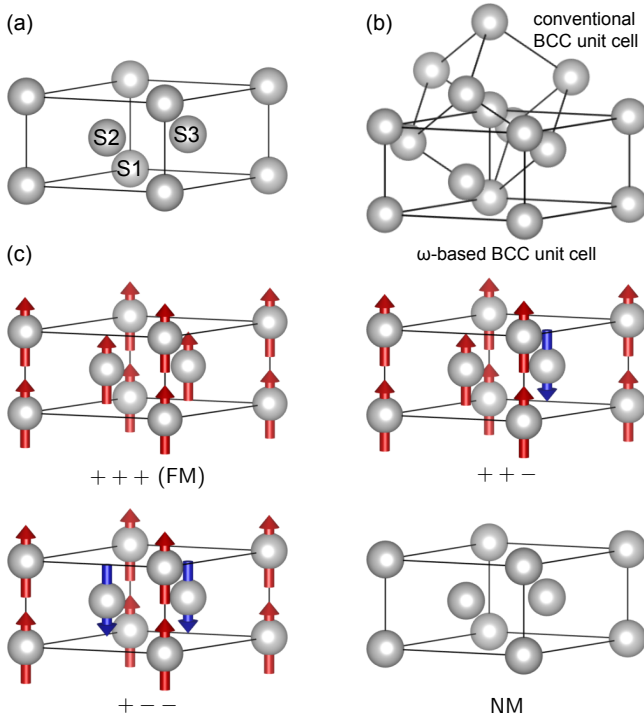


FIG. 1. (Color online) (a) Primitive unit cell of the ω structure. Gray spheres represent atoms. The labels S1, S2, and S3 specify the atoms whose positions are described in the main text. (b) Geometrical relation of the ω -based BCC unit cell to the conventional BCC unit cell. (c) Magnetic states of the ω structure investigated in this study. Up (red) and down (blue) arrows indicate spin-up and spin-down magnetic moments, respectively. Visualization is performed using the VESTA code [29].

dynamical stability of the ω structure for binary alloys composed of the transition elements.

II. COMPUTATIONAL DETAILS

A. ω structure

Figure 1(a) shows the primitive unit cell of the ω structure without considering magnetic configurations. The basis of lattice vectors for the ω structure \mathbf{a}_1 , \mathbf{a}_2 , and \mathbf{a}_3 can be written as,

$$(\mathbf{a}_1 \ \mathbf{a}_2 \ \mathbf{a}_3) = \begin{pmatrix} a_\omega/2 & a_\omega/2 & 0 \\ -\sqrt{3}a_\omega/2 & \sqrt{3}a_\omega/2 & 0 \\ 0 & 0 & c_\omega \end{pmatrix}, \quad (1)$$

where a_ω and c_ω are lattice constants of the ω structure. The ω structure has three atoms, referred to as S1, S2, and S3 hereafter, inside the primitive unit cell. The atomic positions of S1, S2, and S3 are $(0,0,0)$, $(2/3,1/3,1/2)$, and $(1/3,2/3,1/2)$ in fractional coordinates, respectively. The sites S2 and S3 are crystallogra-

TABLE I. Meshes per unit cell to sample Brillouin zones.

	Number of atoms per unit cell	Mesh
BCC	2	$16 \times 16 \times 16$
FCC	4	$12 \times 12 \times 12$
HCP	2	$18 \times 18 \times 12$
ω	3	$12 \times 12 \times 18$

physically equivalent without considering magnetic configurations. The Wyckoff positions are $1a$ for the atom S1 and $2d$ for the atoms S2 and S3.

The BCC structure is related to the ω structure by the orientation relation of $[0001]_\omega || \langle 111 \rangle_{\text{BCC}}$ and $\{11\bar{2}0\}_\omega || \{1\bar{1}0\}_{\text{BCC}}$. The BCC structure can be obtained from the primitive ω unit cell by moving the atoms S2 and S3 to $(2/3, 1/3, 1/3)$ and $(1/3, 2/3, 2/3)$ in fractional coordinates, respectively, and by modifying the lattice constants of the ω structure as,

$$a_\omega = \sqrt{2}a_{\text{BCC}}, \quad (2)$$

$$c_\omega = \sqrt{3}a_{\text{BCC}}/2, \quad (3)$$

where a_{BCC} is the lattice constant of the BCC structure. Figure 1(b) shows the geometrical relation between the conventional and the “ ω -based” unit cell of the BCC structure. From the viewpoint of the ω structure, it is “coherent” with the BCC when the ω structure has the lattice constants that satisfy Eqs. (2) and (3). In other words, if the lattice constants of the ω and the BCC structures exactly satisfy Eqs. (2) and (3), the ω structure can be obtained from the BCC by moving atoms without lattice deformation.

As well as the ω structure, the BCC, FCC, and HCP structures were also investigated for comparison. Four possible magnetic states, including the ferromagnetic (FM) and the nonmagnetic (NM) states, were considered for the ω structure. Figure 1(c) shows the considered magnetic states for the ω structure. For the BCC, FCC, and HCP structures, only the FM and the NM states were considered.

B. Electronic structures and phonons

The plane-wave basis projector augmented wave method [30] was employed in the framework of density-functional theory [31, 32] within the generalized gradient approximation (GGA) in the Perdew-Burke-Ernzerhof (PBE) form [33] as implemented in the VASP code [34–36]. A plane-wave energy cutoff of 400 eV was used. The Brillouin zones were sampled by Γ centered meshes according to crystal structures as shown in Table I, and the Methfessel-Paxton scheme [37] with a smearing width of 0.4 eV was employed. Total energies were minimized until the energy convergences to be less than 10^{-8} eV. Lattice parameters were optimized under zero external

TABLE II. Obtained magnetic states with nonzero magnetic moments.

	Magnetic state	Element
BCC	FM	Mn, Fe, Co, Ni, Rh, Ir
FCC	FM	Fe, Co, Ni
HCP	FM	Co, Ni
ω	FM	Fe, Co, Ni
	++-	Fe
	+- -	Fe

stress. Magnetic moments on atoms were determined from the electron density in corresponding Voronoi cells.

Phonon frequencies of the ω structures were calculated based on the harmonic approximation for a lattice Hamiltonian using the finite-displacement method. Atomic displacements of 0.01 Å for the $2 \times 2 \times 4$ supercell of the ω unit cell (including 48 atoms) were used to calculate the second-order force constants. The PHONOPY code [38, 39] was used for these phonon calculations.

III. RESULTS AND DISCUSSION

A. Energetics for the ω structure of transition elements

Table II summarizes the magnetic states with nonzero magnetic moments found in the present calculations. Most of the nonzero magnetic moments are found for the 3d transition elements. The FM ω structure is obtained for Fe, Co, and Ni. The ω Fe has also the ++- and the +- - magnetic states, which are described in Fig. 1(c). Magnetic moments converge to zero for the rest of the elements even for spin-unrestricted calculations.

Table III shows calculated energies, lattice constants, and volumes of the NM ω structure for 27 transition elements, and Table IV shows the values for the other magnetic states. Table V gives calculated magnetic moments on atoms. Volumes of the magnetic states with nonzero magnetic moments are larger than that in the NM state. The FM ω structure for Co and Ni are 285 and 39 meV/atom lower in energy than the NM state, respectively. For Fe, the +- - magnetic state is the lowest in energy among the obtained magnetic states. The FM ω Fe is 32 meV/atom higher in energy than the +- - magnetic state and hence is thermodynamically less favorable. The NM ω Fe, which is 90 meV/atom higher in energy than the +- - state, has the highest energy among the obtained magnetic states.

Table VI summarizes the energies relative to that of the NM FCC structure, and Fig. 2 visualizes the result. For the NM state, most of the elements in the same groups show the same energy sequences for the inves-

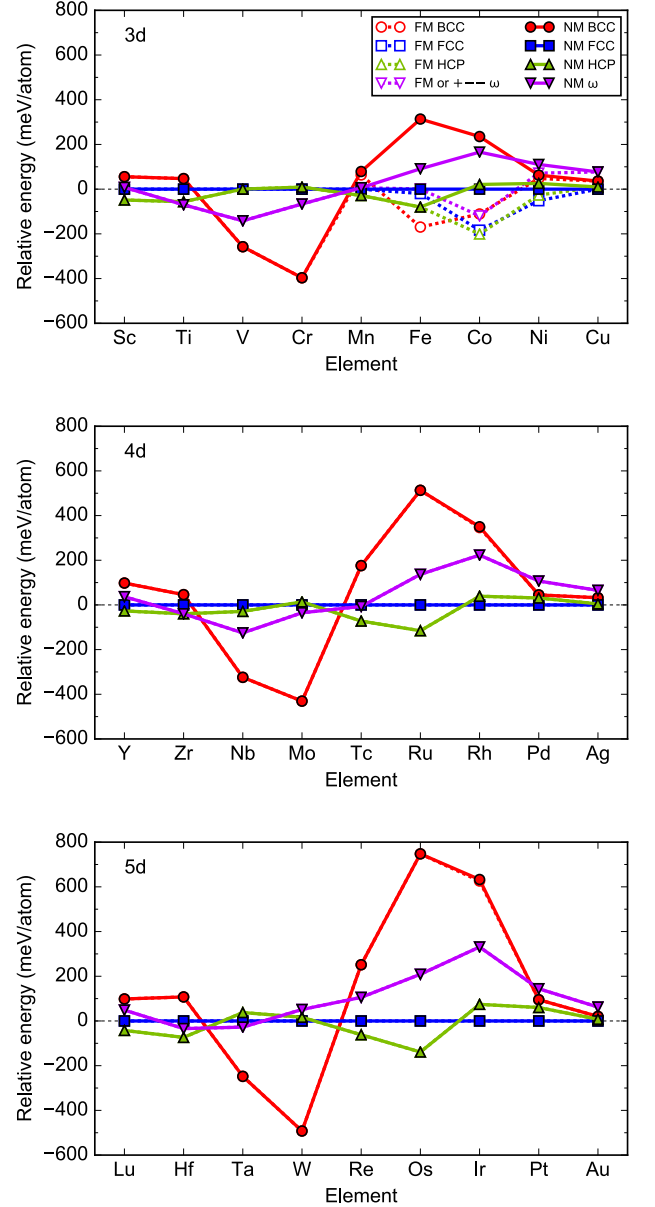


FIG. 2. (Color online) Calculated energies of the transition elements relative to that of the NM FCC structure. Red circle, blue square, green triangle, and purple inverse triangle symbols denote the BCC, FCC, HCP, and ω structures, respectively. Filled symbols connected by solid lines indicate the NM state, while open symbols connected by dashed lines are for the magnetic state that has the lowest energy among the investigated ones. Note that the +- - ω structure is the lowest in energy only for Fe, and the FM state is the lowest in energy for the other systems. The lines are guides for the eyes.

TABLE III. Calculated energies, lattice constants, and volumes of the NM ω structures for the transition elements. The energies are relative to that of the NM FCC structure.

	Relative energy (meV/atom)	a_ω (Å)	c_ω (Å)	Volume (Å ³ /atom)
Sc	8	5.098	3.202	24.02
Ti	-70	4.542	2.824	16.82
V	-142	4.448	2.341	13.37
Cr	-66	4.229	2.262	11.68
Mn	6	3.887	2.448	10.68
Fe	91	3.850	2.418	10.35
Co	166	3.899	2.390	10.49
Ni	111	3.987	2.397	11.00
Cu	77	4.126	2.472	12.15
Y	37	5.638	3.527	32.36
Zr	-40	5.036	3.149	23.06
Nb	-125	4.876	2.678	18.38
Mo	-35	4.668	2.538	15.97
Tc	-7	4.291	2.716	14.44
Ru	137	4.252	2.680	13.99
Rh	223	4.329	2.655	14.37
Pd	107	4.493	2.676	15.59
Ag	65	4.721	2.820	18.15
Lu	49	5.433	3.413	29.08
Hf	-34	4.963	3.096	22.01
Ta	-28	4.853	2.709	18.42
W	51	4.678	2.590	16.36
Re	106	4.375	2.744	15.16
Os	209	4.320	2.723	14.67
Ir	331	4.381	2.703	14.98
Pt	144	4.526	2.704	15.99
Au	62	4.748	2.815	18.32

tigated crystal structures. For example, the sequence for the group 8 elements (Fe, Ru, and Os) in the NM state is HCP \rightarrow FCC \rightarrow ω \rightarrow BCC in order of increasing energy. This result indicates that relative energies are roughly determined from the occupation number for d orbitals for these crystal structures. This tendency has already been pointed out for the BCC, FCC, and HCP structures [40]. The present calculations reveal that the ω structure also follows this rule. The NM ω structure tends to be lower in energy than the NM FCC structure for early transition elements except for those in the group 3 (Sc, Y, and Lu) and to be higher for late transition elements. This tendency is similar to that for the NM BCC structure. The NM ω structure is also lower in energy than the NM BCC for the elements in the groups 3, 4, 7, 8, and 9 and higher for the elements in the other groups. For the elements in the groups 5 and 6 except for W, the NM ω structure is the second lowest in energy among the investigated crystal structures.

For the group 4 elements, the relative energies of the ω structure are low compared with the elements in the other groups. The energies of the ω structure relative to those of the HCP, which is observed in experiments at ambient

TABLE IV. Calculated energies, lattice constants, and volumes of the ω structure for the transition elements in the magnetic states with nonzero magnetic moments. The energies are relative to that of the NM FCC structure.

		Relative energy (meV/atom)	a_ω (Å)	c_ω (Å)	Volume (Å ³ /atom)
Fe	FM	33	4.177	2.375	11.96
	++-	35	3.992	2.386	10.97
	+- -	1	3.970	2.397	10.91
	NM	91	3.850	2.418	10.35
Co	FM	-120	3.953	2.434	10.98
	NM	166	3.899	2.390	10.49
Ni	FM	72	3.989	2.414	11.09
	NM	111	3.987	2.397	11.00

TABLE V. Calculated magnetic moments on atoms for the ω structure. Note that the sites S2 and S3 are crystallographically equivalent for the FM and the +- - states but not for the +-+ state. The equivalent values are shown in parentheses.

		Magnetic moment (μ_B)		
		S1	S2	S3
Fe	FM	2.59	2.45	(2.45)
	++-	1.56	1.72	-1.90
	+- -	1.69	-1.63	(-1.63)
Co	FM	1.60	1.67	(1.67)
Ni	FM	0.62	0.66	(0.66)

temperature and pressure, are -13, 0, and 39 meV/atom for Ti, Zr, and Hf, respectively. These small energy differences indicate that the ω structure is thermodynamically favorable for the group 4 elements. The ω structure of the group 4 elements is actually observed in experiments [2-4]. Note that for Ti, our computational result shows that the ω structure is lower in energy than the HCP structure. This result has also been shown in a previous report [27] and hence is correct at least within DFT calculations using the GGA PBE functional.

The +- - ω Fe is 170 meV/atom higher in energy than the FM BCC Fe, which is observed in experiments at ambient temperature and pressure. This energy difference between the ω structure and the state in experiments is much larger than those for the group 4 elements, which implies that the ω structure of Fe is thermodynamically more difficult to be formed than that of the group 4 elements. In contrast, several experimental reports have claimed that the ω structure can be formed in Fe-based alloys [16, 17]. In these experiments, the ω structure has been observed at twin boundaries of the BCC or as precipitates in the BCC matrix. Such kinds of structural imperfections and/or coherent stress at the interfaces are

TABLE VI. Calculated energies of the transition elements relative to that of the NM FCC structure in meV/atom.

	BCC		FCC		HCP		ω			
	NM	FM	NM	FM	NM	FM	NM	+ - -	+ + -	FM
Sc	56		0		-49		8			
Ti	47		0		-56		-70			
V	-258		0		0		-142			
Cr	-397		0		9		-66			
Mn	79	64	0		-29		6			
Fe	314	-170	0	-20	-80		91	1	35	33
Co	235	-111	0	-184	21	-201	166			-120
Ni	63	48	0	-52	26	-26	111			72
Cu	36		0		10		77			
Y	98		0		-27		37			
Zr	46		0		-40		-40			
Nb	-324		0		-29		-125			
Mo	-431		0		14		-35			
Tc	176		0		-72		-7			
Ru	513		0		-116		137			
Rh	350	346	0		39		223			
Pd	45		0		31		107			
Ag	32		0		5		65			
Lu	98		0		-42		49			
Hf	107		0		-74		-34			
Ta	-248		0		38		-28			
W	-492		0		17		51			
Re	251		0		-62		106			
Os	748		0		-139		209			
Ir	633	626	0		74		331			
Pt	95		0		60		144			
Au	20		0		8		62			

maybe required to form the ω Fe. Effect of solute elements is another possible reason for the formation of the ω structure in the Fe-based alloys. If the solute elements thermodynamically stabilize the ω structure more than the BCC, the Fe-based alloys may prefer to form the ω structure. As mentioned above, the NM ω structure is lower in energy than the NM BCC for the elements in the groups 3, 4, 7, 8, and 9, and hence these elements are expected to stabilize the ω structure more than the BCC. In addition, the FM ω Co is -9 meV/atom lower in energy than the FM BCC Co, and hence Co is also expected to stabilize the ω structure more than the BCC.

Figure 3 summarizes the calculated volumes relative to those of the NM FCC structure. For the NM state, most of the elements in the same groups show the same volume sequences for the investigated crystal structure, similarly to the case of the relative energies. The NM ω structure tends to be smaller in volume than the NM FCC structure for early transition elements and to be larger for late transition elements.

Figure 4 shows the ratios of calculated lattice constants of the NM ω structure to that of the NM BCC structure. Dashed horizontal lines indicate the values coherent with the BCC structure described in Eqs. (2) and (3). The

values for the elements in the groups 5 and 6 are largely deviated from the coherent ones compared with the other transition elements. Therefore, the ω structure may be largely deformed for the elements in the groups 5 and 6 when it is coherent with the BCC structure.

B. Mechanical stability of the ω structure

Figures 5, 6, and 7 show calculated phonon dispersion relations of the NM ω structure for the transition elements. The elements in the same groups show similar shapes of the phonon dispersion relations. Heavier elements in the same groups tend to have smaller absolute values of phonon frequencies.

The NM ω structure of Ti, Mn, Fe, Co, Zr, Tc, Hf, and Re has no imaginary modes and hence is mechanically stable. The ω structure of Ti and Zr is actually observed at ambient temperature and pressure [2]. Although Hf is included in the group 4 as well as Ti and Zr, the ω Hf has not been observed in experiments at ambient temperature and pressure [3, 4]. The present calculations elucidate that this is not because the ω Hf is mechanically unstable.

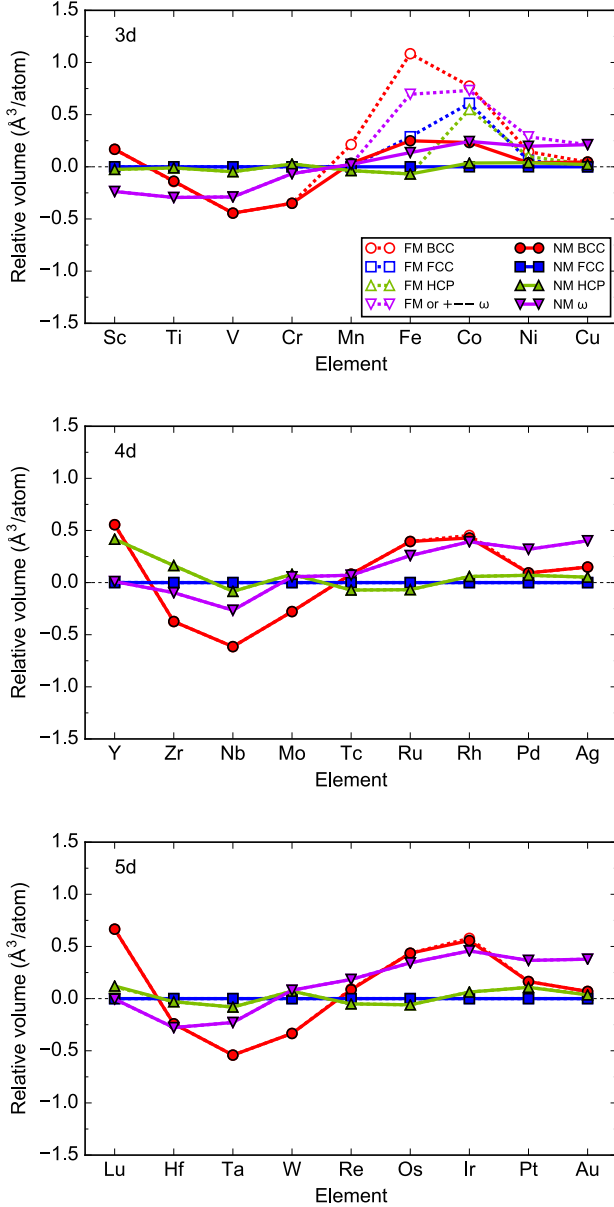


FIG. 3. (Color online) Calculated volumes of the transition elements relative to that for the NM FCC structure. Notations are the same as Fig. 2.

To our best knowledge, the ω structure has not been reported for the group 7 elements (Mn, Tc, and Re), while the ω structure for these elements is mechanically stable. For the group 7 elements, the energies of the ω structure relative to the HCP, which is the lowest in energy among the investigated crystal structures, are 35, 65, and 167 meV/atom for Mn, Tc, and Re, respectively. These energy differences are higher than those for the group 4 elements. In experiments, furthermore, Mn forms the antiferromagnetic (AFM) A12 structure as the equilibrium state at 4.2 K and at ambient pressure

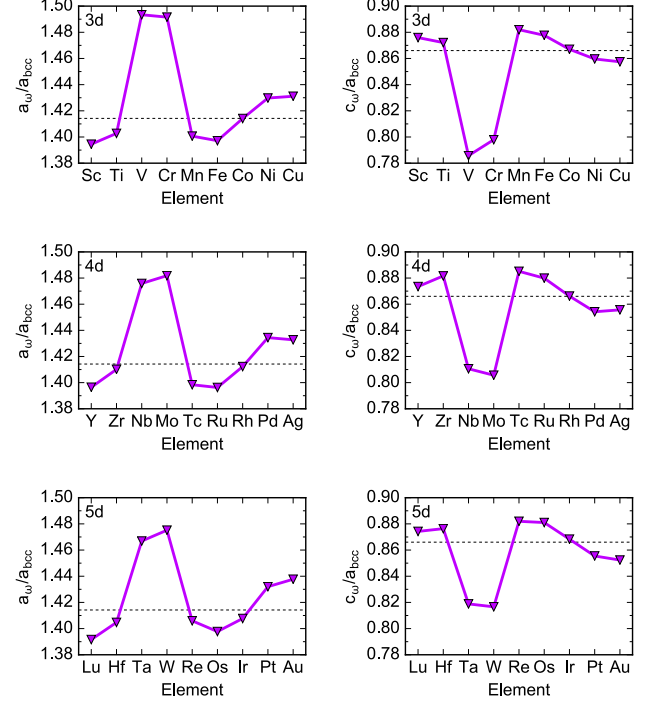


FIG. 4. (Color online) Ratios of calculated lattice constants of the NM ω structure to that of the NM BCC structure. The left and the right panels are for a_ω/a_{BCC} and c_ω/a_{BCC} , respectively. Dashed horizontal lines indicate the values coherent with the BCC structure described in Eqs. (2) and (3). Lines are guides for the eyes.

[41]. First-principles calculations suggest that the energy of the AFM A12 structure is 60 meV/atom lower in energy than the NM HCP [42]. As a result, we can estimate that the ω Mn is 95 meV/atom higher in energy than the experimental equilibrium state. These results indicate that although the ω structure of the group 7 elements is mechanically stable, they are thermodynamically less favorable than other crystal structures compared with the group 4 elements. Therefore, the ω structure of the group 7 elements is probably more difficult to be formed in experiments than that of the group 4 elements.

The ω structure of the elements in the groups 5 and 6 has phonon modes with imaginary frequencies and hence are mechanically unstable. Several experimental reports, however, have claimed that the ω structure can be formed in Ta and Mo [14, 15]. In these experiments, the ω structure has been observed in the matrix of the BCC structure, and hence structural imperfections and/or coherent stress at the interfaces between the ω and the BCC structures may affect the formation of the ω structure.

Figure 8 shows calculated phonon dispersion relations of the ω structure in the obtained magnetic states for Fe, Co, and Ni. Fe shows large differences among the magnetic states. The FM and the $++-\omega$ Fe have phonon modes with imaginary frequencies and hence are mechan-

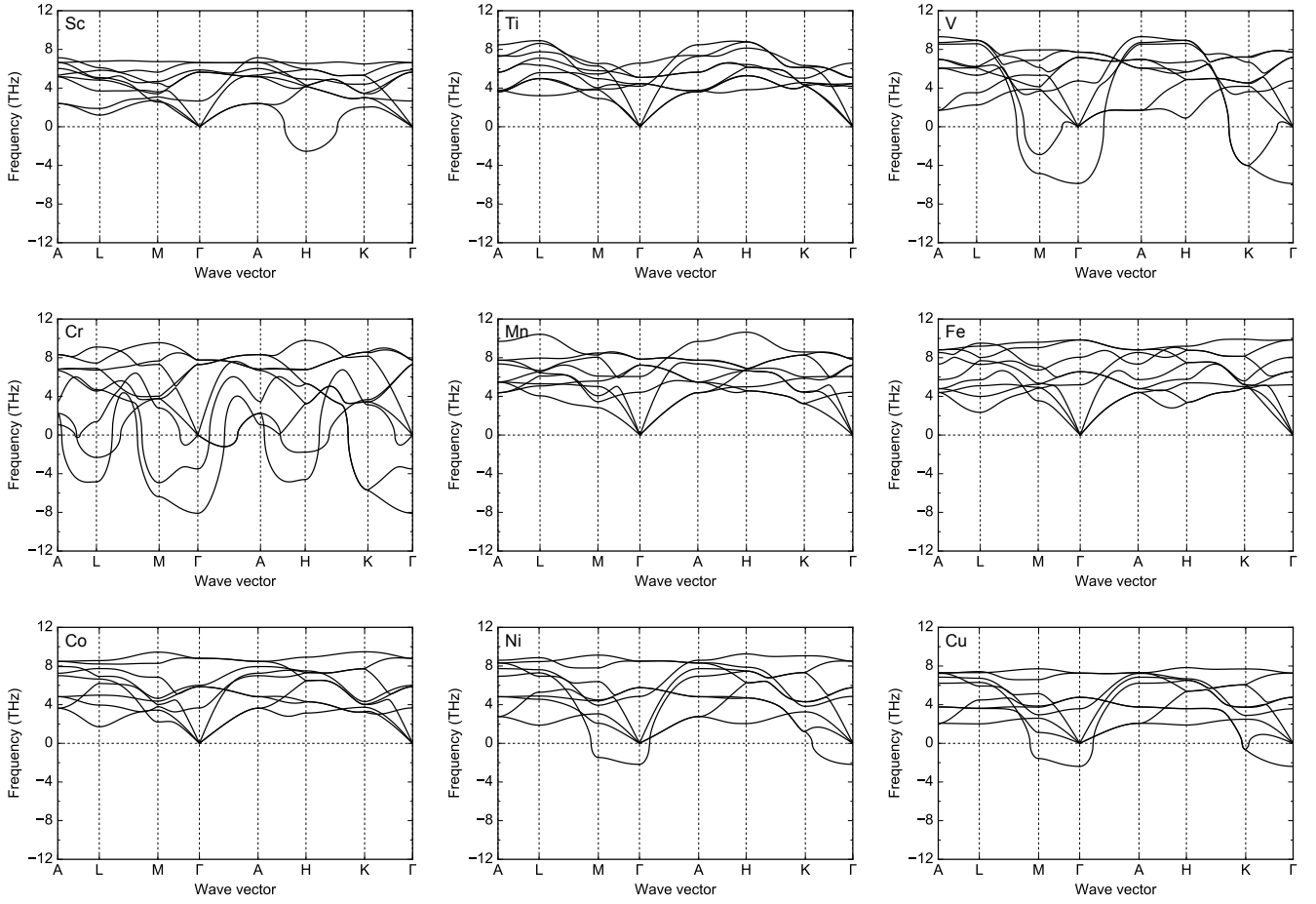


FIG. 5. Calculated phonon dispersion relations of the NM ω structure for the 3d transition elements. Imaginary phonon frequencies are shown by negative values.

ically unstable. In contrast, the $+ - -$ and the NM ω Fe have no phonon modes with imaginary frequencies and hence are mechanically stable. It has been well investigated that mechanical stability of the BCC and FCC Fe largely depend on their magnetic states such as NM, FM, and PM ones [28, 43, 44]. The present result shows that magnetic states also affect the mechanical stability of the ω Fe. As shown above, the $+ - -$ state is also the lowest in energy among the magnetic states for the ω structure, and hence the ω Fe is expected to show the $+ - -$ state if it is formed.

The FM ω Co has a phonon mode with an imaginary frequency at the Γ point (see the inset in Fig. 8), while the NM ω Co has no phonon modes with imaginary frequencies. Since the absolute value of the imaginary phonon frequency is very small for the FM ω Co, it is difficult to conclude whether the FM ω Co is actually mechanically unstable or not at the present moment. The ω Ni does not show qualitative differences between the FM and the NM states.

C. Energetics for the ω structure of binary alloys

The ω structure is frequently observed in alloys based on the group 4 elements [1, 5–13]. It should be, therefore, interesting to investigate energetics of such alloys.

Since the occupation number for d orbitals roughly determines the relative energies of the crystal structures of our interest, we can approximately estimate the energies of a binary alloy $A_{1-x}B_x$ by linear interpolation as,

$$E_s(A_{1-x}B_x) \approx (1-x)E_s(A) + xE_s(B), \quad (4)$$

where E represents the energy per atom, the symbols A and B represent the elements in the alloy, x represents the concentration of the element B, and the subscript s specifies the crystal structure. Note that any kinds of atomic orderings are not considered in this equation. The interpolated energy is actually the same as that of the phase-separation state of the same crystal structure. Nevertheless, this estimation is probably useful to qualitatively discuss thermodynamical stability of crystal structures for alloys with specific compositions.

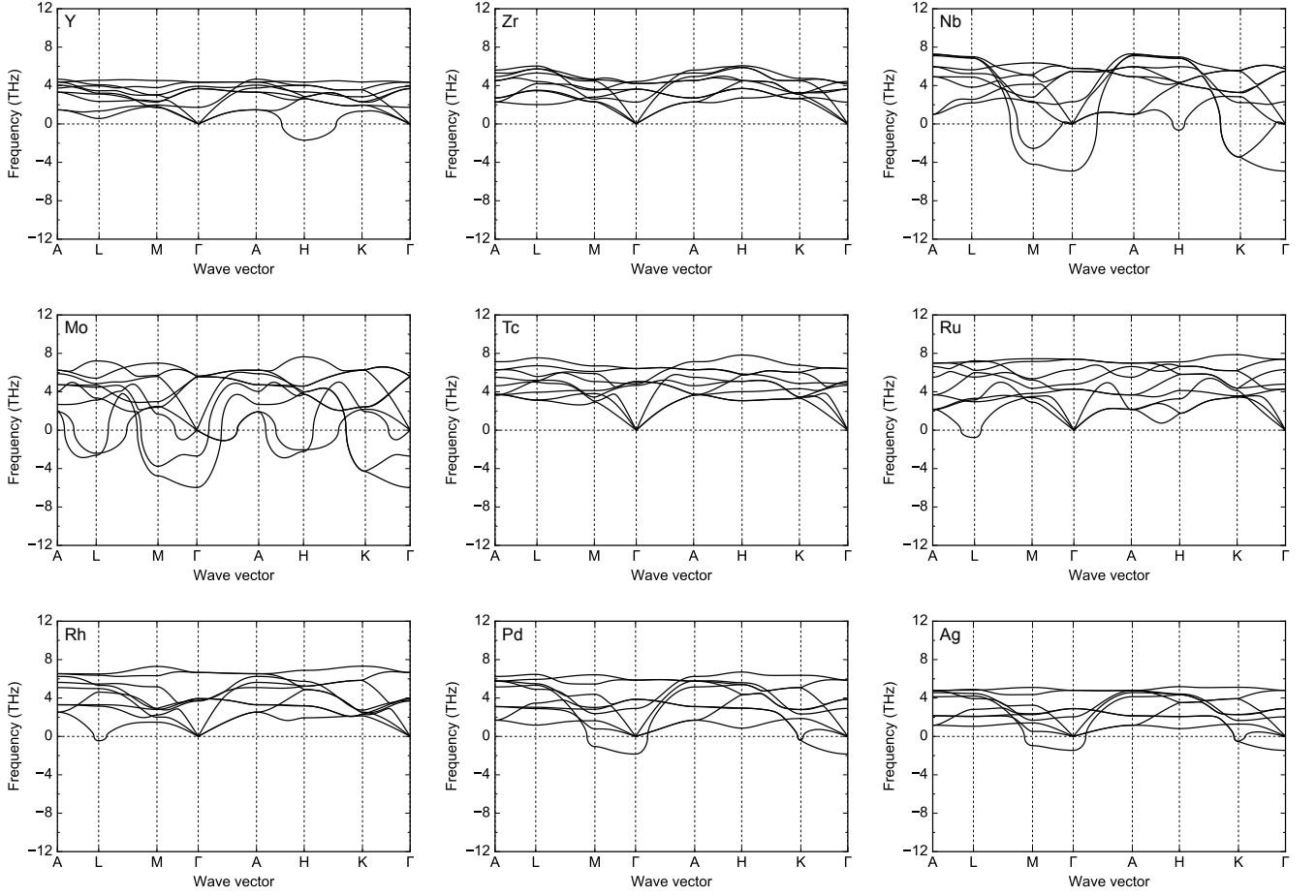


FIG. 6. The same as Fig. 5 but for the 4d transition elements. For Tc, which has no stable isotopes, we use the relative atomic mass of ^{99}Tc , 98.906, to calculate phonon dispersion relations. Note that differences of the atomic mass only scale phonon frequencies.

Figure 9 shows estimated energies of binary alloys composed of the elements in the group 4 and those in the groups 5 and 6. Most of the binary alloys shown in the figure have the concentration range where the ω structure is the lowest in energy among the investigated crystal structures. The group 4 elements are richer in these concentration ranges. In experiments, the ω structure is observed for the alloys based on the group 4 elements with those in the groups 5 and 6 in the concentration ranges where the group 4 elements are richer [1, 5, 7, 8, 10–13]. This experimental fact implies that the ω structure is relatively favorable for these alloys in the concentration ranges with rich group 4 elements. The present computational result corresponds to this experimental fact.

The ω structure is favorable for these alloys because of the following reason. The HCP and the ω structures have almost the same energies for the group 4 elements, while the HCP structure is substantially higher in energy than the ω structure for the elements in the groups 5 and 6 except for W. For the alloys composed of the group 4

elements and those in the groups 5 and 6, therefore, the ω structure is estimated to be lower in energy than the HCP. The ω structure is substantially lower in energy than the HCP only for the elements in the groups 5 and 6, and hence this tendency is specific for the alloys composed of the group 4 elements and those in the groups 5 and 6.

Note that even if the ω structure is the lowest in energy at a specific concentration, this does not mean that the ω structure is the equilibrium state at this concentration. When we consider a phase-separation state composed of two different crystal structures with different compositions, this phase-separation state can be lower in energy than the ω structure. For example, the estimated relative energy of the NM ω $\text{Ti}_{0.75}\text{V}_{0.25}$ to the NM FCC is -88 meV/atom, while the mixture of 75 % NM HCP Ti and 25 % NM BCC V has the relative energy of -106 meV/atom. In experiments, the ω structure in Ti-V alloys is actually thermodynamically metastable and finally decomposes into the HCP and the BCC structures

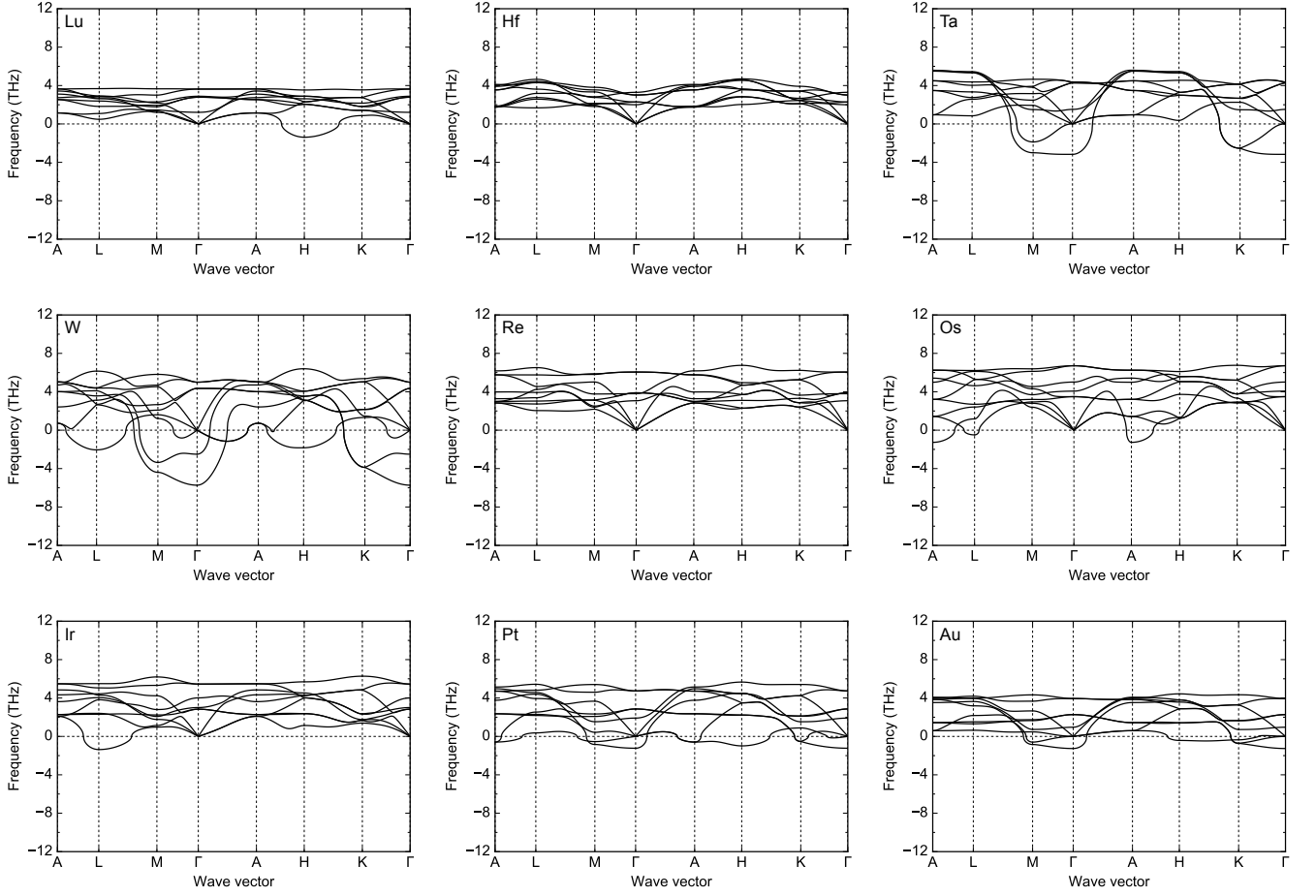


FIG. 7. The same as Fig. 5 but for the 5d transition elements.

with different concentrations of V atoms after sufficiently long-time aging [45].

IV. CONCLUSION

Properties of the ω structure are systematically investigated for 27 transition elements from the viewpoints of thermodynamical and mechanical stability using first-principles calculations. The mechanical stability is investigated in terms of phonon frequencies.

The occupation number for d orbitals roughly determines relative energy and volume of the NM ω structure as well as the other investigated crystal structures (BCC, FCC, and HCP). For the group 4 elements (Ti, Zr, and Hf), the ω structure is thermodynamically favorable and is mechanically stable. For the group 7 elements (Mn, Tc, and Re), the ω structure is also mechanically stable, but they are thermodynamically less favorable compared with the group 4 elements. For the elements in the groups 5 and 6, the lattice constants of the ω structure are largely deviated from the values coherent with the

BCC structure.

Several 3d transition elements, namely Fe, Co, and Ni, have the ω structure with nonzero magnetic moments. For the ω Fe, the $+-$ state is the lowest in energy among the magnetic states and is also mechanically stable. Co and Ni show the FM ω structure, and it is lower in energy than the NM state.

Energies of binary alloys composed of the elements in the group 4 and those in the groups 5 and 6 are estimated by linear interpolation. Most of these alloys have a concentration range where the ω structure is the lowest in energy among the investigated crystal structures. The group 4 elements are richer in these concentration ranges. This result corresponds to the following experimental fact; for the alloys composed of the group 4 and those in the groups 5 and 6, the ω structure is observed in concentration ranges where the group 4 elements are richer.

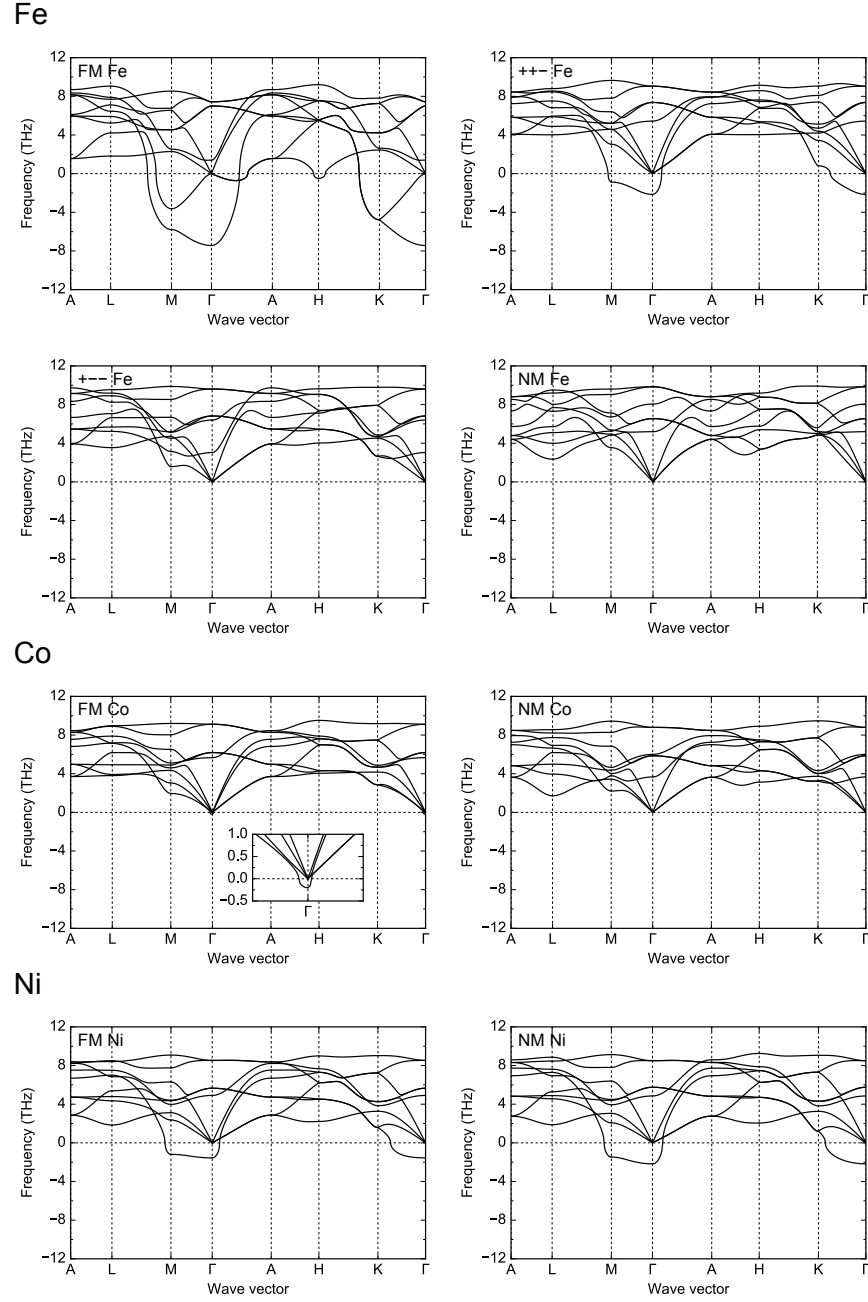


FIG. 8. Calculated phonon dispersion relations of the ω structure in the obtained magnetic states for Fe, Co, and Ni. The inset for the FM ω Co is the magnified view around the Γ point, which is shown to confirm a phonon mode with an imaginary frequency.

ACKNOWLEDGMENTS

Funding by the Ministry of Education, Culture, Sports, Science and Technology (MEXT), Japan, through Ele-

ments Strategy Initiative for Structural Materials (ES-ISM) of Kyoto University, is gratefully acknowledged.

[1] P. Frost, W. Parris, L. Hirsch, J. Doig, and C. Schwartz, Trans. Am. Soc. Met. **46**, 231 (1954).

[2] J. C. Jamieson, Science **140**, 72 (1963).

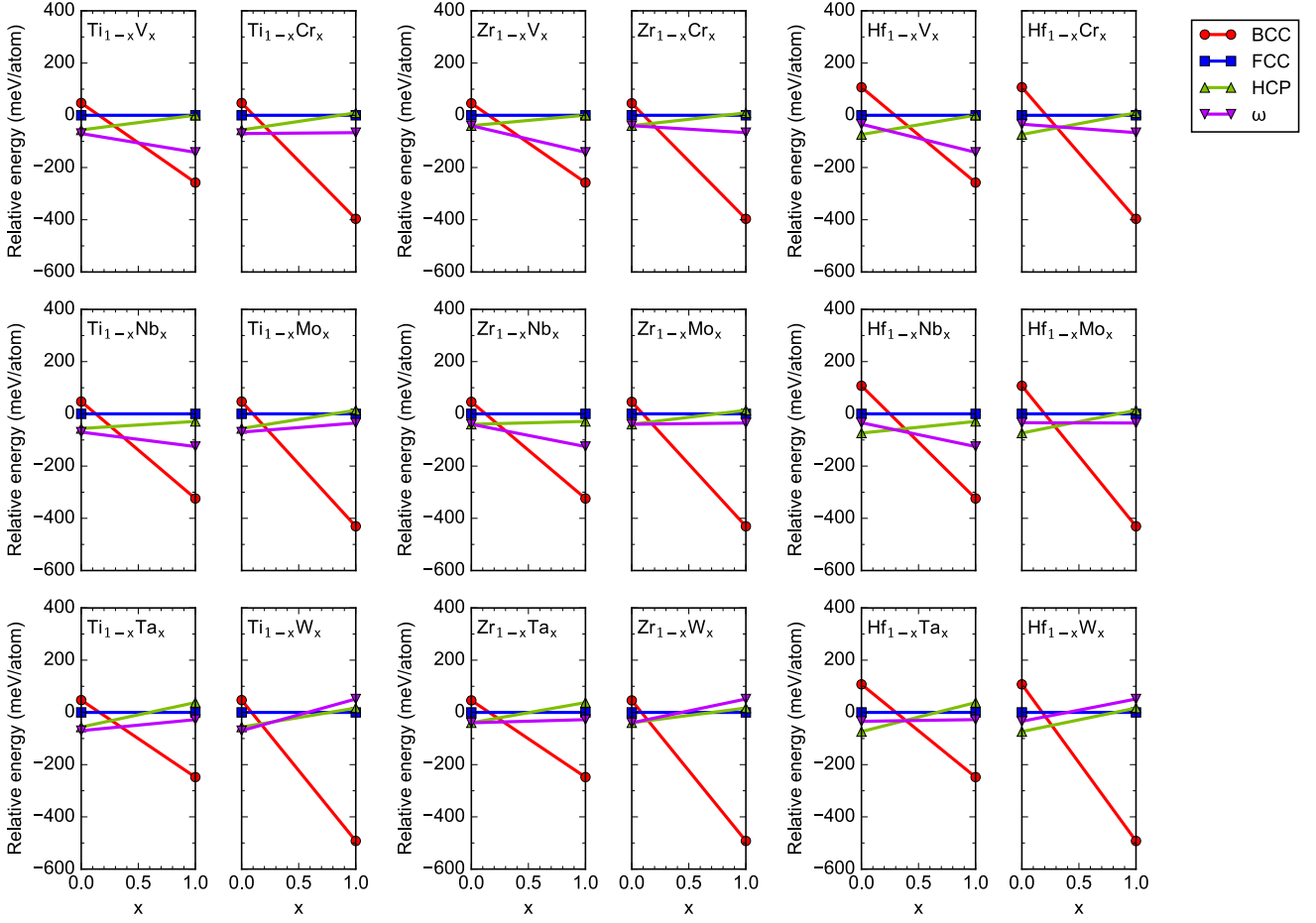


FIG. 9. Estimated energies of the binary alloys composed of the elements in the group 4 and those in the groups 5 and 6. The energies are relative to that of the NM FCC structure for each alloy. The left side of each figure is for the elements in the group 4, and the right side is for the elements in the groups 5 and 6.

- [3] H. Xia, G. Parthasarathy, H. Luo, Y. K. Vohra, and A. L. Ruoff, *Phys. Rev. B* **42**, 6736 (1990).
- [4] K. K. Pandey, J. Gyanchandani, M. Somayazulu, G. K. Dey, S. M. Sharma, and S. K. Sikka, *J. Appl. Phys.* **115**, 233513 (2014).
- [5] J. Silcock, *Acta Metall.* **6**, 481 (1958).
- [6] S. L. Sass, *Acta Metall.* **17**, 813 (1969).
- [7] B. Hickman, *Trans. Metall. Soc. AIME* **245**, 1329 (1969).
- [8] C. Cui and D. Ping, *J. Alloys Compd.* **471**, 248 (2009).
- [9] S. Wu, D. Ping, Y. Yamabe-Mitarai, W. Xiao, Y. Yang, Q. Hu, G. Li, and R. Yang, *Acta Mater.* **62**, 122 (2014).
- [10] D. Ping, C. Cui, F. Yin, and Y. Yamabe-Mitarai, *Scr. Mater.* **54**, 1305 (2006).
- [11] B. A. Hatt, J. A. Roberts, and G. I. Williams, *Nature* **180**, 1406 (1957).
- [12] B. Hatt and J. Roberts, *Acta Metall.* **8**, 575 (1960).
- [13] W. Jackson, A. Perkins, and R. Hehemann, *Metall. Trans.* **1**, 2014 (1970).
- [14] L. Hsiung and D. Lassila, *Acta Mater.* **48**, 4851 (2000).
- [15] G. Cheng, H. Yuan, W. Jian, W. Xu, P. Millett, and Y. Zhu, *Scr. Mater.* **68**, 130 (2013).
- [16] D. Ping and W. Geng, *Mater. Chem. Phys.* **139**, 830 (2013).
- [17] T. Liu, D. Zhang, Q. Liu, Y. Zheng, Y. Su, X. Zhao, J. Yin, M. Song, and D. Ping, *Sci. Rep.* **5**, 15331 (2015).
- [18] A. Prasetyo, F. Reynaud, and H. Warlimont, *Acta Metall.* **24**, 1009 (1976).
- [19] A. Prasetyo, F. Reynaud, and H. Warlimont, *Acta Metall.* **24**, 651 (1976).
- [20] P. Georgopoulos and J. Cohen, *Acta Metall.* **29**, 1535 (1981).
- [21] A. Yedneral and M. Perkas, *Fiz. Met. Metalloved.* **33**, 315 (1972).
- [22] J. Lecomte, C. Servant, and G. Cizeron, *J. Mater. Sci.* **20**, 3339 (1985).
- [23] C. Djega-Mariadassou, L. Bessais, and C. Servant, *Phys. Rev. B* **51**, 8830 (1995).
- [24] S. Sikka, Y. Vohra, and R. Chidambaram, *Prog. Mater. Sci.* **27**, 245 (1982).
- [25] M. P. Usikov and V. A. Zilbershtein, *Phys. Status Solidi A* **19**, 53 (1973).
- [26] D. R. Trinkle, R. G. Hennig, S. G. Srinivasan, D. M. Hatch, M. D. Jones, H. T. Stokes, R. C. Albers, and J. W. Wilkins, *Phys. Rev. Lett.* **91**, 025701 (2003).

- [27] A. Togo and I. Tanaka, Phys. Rev. B **87**, 184104 (2013).
- [28] Y. Ikeda, A. Seko, A. Togo, and I. Tanaka, Phys. Rev. B **90**, 134106 (2014).
- [29] K. Momma and F. Izumi, J. Appl. Crystallogr. **44**, 1272 (2011).
- [30] P. E. Blöchl, Phys. Rev. B **50**, 17953 (1994).
- [31] P. Hohenberg and W. Kohn, Phys. Rev. **136**, B864 (1964).
- [32] W. Kohn and L. J. Sham, Phys. Rev. **140**, A1133 (1965).
- [33] J. P. Perdew, K. Burke, and M. Ernzerhof, Phys. Rev. Lett. **77**, 3865 (1996).
- [34] G. Kresse, J. Non-Cryst. Solids **192-193**, 222 (1995).
- [35] G. Kresse and J. Furthmüller, Comput. Mater. Sci. **6**, 15 (1996).
- [36] G. Kresse and D. Joubert, Phys. Rev. B **59**, 1758 (1999).
- [37] M. Methfessel and A. T. Paxton, Phys. Rev. B **40**, 3616 (1989).
- [38] A. Togo and I. Tanaka, Scr. Mater. **108**, 1 (2015).
- [39] A. Togo, F. Oba, and I. Tanaka, Phys. Rev. B **78**, 134106 (2008).
- [40] H. L. Skriver, Phys. Rev. B **31**, 1909 (1985).
- [41] C. G. Shull and M. K. Wilkinson, Rev. Mod. Phys. **25**, 100 (1953).
- [42] J. Hafner and D. Hobbs, Phys. Rev. B **68**, 014408 (2003).
- [43] H. C. Hsueh, J. Crain, G. Y. Guo, H. Y. Chen, C. C. Lee, K. P. Chang, and H. L. Shih, Phys. Rev. B **66**, 052420 (2002).
- [44] F. Körmann, A. Dick, B. Grabowski, T. Hickel, and J. Neugebauer, Phys. Rev. B **85**, 125104 (2012).
- [45] B. Hickman, J. Inst. Met. **96**, 330 (1968).